Journal of Inflammation Research

Dovepress
Taylor & Francis Group

Open Access Full Text Article

CLINICAL TRIAL REPORT

In vitro Validation of a Novel Disposable Remover to Remove Activated Leukocytes Generated During Cardiopulmonary Bypass: A Pilot Study

Yuling Zheng[1,2], Ying Ran[3], Juan Wu[1], Ping Yang[1], Xinyi Liao[1], Jie Zhang[4], Wentong Meng[5], Daming Gou[6], Li Li[7], Lei Du[1], Jing Lin[1]

[1]Department of Anesthesiology, West China Hospital, Sichuan University & West China Research Unit, Chinese Academy of Medical Sciences, Chengdu, Sichuan, 610041, People's Republic of China; [2]Department of Anesthesiology, Zunyi Maternal and Child Health Care Hospital, Zunyi, Guizhou, 563000, People's Republic of China; [3]Department of Anesthesiology, Zunyi Medical University, Zunyi, Guizhou, 563003, People's Republic of China; [4]Key Laboratory of Transplant Engineering and Immunology, Ministry of Health, West China Hospital, Sichuan University, Chengdu, Sichuan, 610041, People's Republic of China; [5]Laboratory of Stem Cell Biology, State Key Laboratory of Biotherapy, West China Hospital, Sichuan University, Chengdu, Sichuan, 610041, People's Republic of China; [6]Department of Anesthesiology, KweiChow Moutai Hospital, Renhuai, Guizhou, 564501, People's Republic of China; [7]Institute of Blood Transfusion, Chinese Academy of Medical Sciences, Peking Union Medical College, Chengdu, Sichuan, 610052, People's Republic of China

Correspondence: Jing Lin, Department of Anesthesiology, West China Hospital, Sichuan University, No. 37 Guoxue Alley, Wuhou District, Chengdu, Sichuan, 610041, People's Republic of China, Tel +86 2885423593, Email linjing@wchscu.cn

Background: Cardiopulmonary bypass (CPB) is associated with activation of pro-inflammatory cells, which infiltrate tissues and cause injury. Here we explored a novel disposable remover to remove inflammatory leukocytes in order to reduce risk of complications after CPB. This is a substudy within a previously registered clinical trial (NCT05400356) that aims to validate a novel disposable remover to remove activated leukocytes generated during CPB.

Methods: The device contains an enhanced biocompatible leukocyte membrane (Chinese patent CN202310822538.X) coated with RGD peptide (Arg-Gly-Asp), which binds to specific polypeptide groups on activated leukocytes, leading to their affinity-based adsorption. The device was integrated into a closed extracorporeal circuit containing a blood reservoir, roller pump, and tubes. Blood from seven patients (150 mL per patient) was driven through the circuit for 10 min at 300 mL/min. Counts of leukocytes and their surface molecules were examined before circulation and after 2.5, 5, 7.5, and 10 min of circulation. The types and morphology of blood cells captured on the filter membrane were also examined.

Results: Counts of neutrophils and neutrophils expressing the activation markers CD11b, CD54, CD64 or CD181 decreased rapidly by 36–39% during the first 2.5 min of circulation, after which their counts decreased more slowly. In contrast, counts of monocytes or lymphocytes did not change significantly during circulation. After use, the membrane was still smooth and intact, and it contained substantial numbers of intact activated leukocytes, based on immunostaining against activated cells and scanning electron microscopy. Smears of blood samples before and after circulation showed no significant differences in each leukocyte morphology.

Conclusion: This novel disposable remover can preferentially remove activated neutrophils from blood ex vivo, with minimal apparent impact on other leukocytes and blood components.

Trial Registration: This substudy is part of a prospective cohort study registered at the Clinical Trials Registry (NCT05400356) on 27 May 2022.

Keywords: cardiopulmonary bypass, systemic inflammatory response syndrome, leukocyte filter, inflammatory cell, flow cytometry

Introduction

Cardiopulmonary bypass (CPB) during cardiac surgery strongly increases risk of postoperative morbidity and mortality, primarily because it can induce systemic inflammatory response syndrome (SIRS),[1] which involves activation of leukocytes[2,3] that infiltrate into tissues,[4] where they secrete excessive amounts of pro-inflammatory cytokines[5,6] that cause inflammatory reactions. In the past, glucocorticoids were widely used to dampen these inflammatory responses, yet

Received: 18 December 2024
Accepted: 4 April 2025
Published: 18 April 2025

they do not improve prognosis after on-pump cardiac surgery.[7,8] In another approach, the CytoSorb has been developed to remove pro-inflammatory factors from blood, but in several clinical trials, it failed to improve prognosis of patients who experience SIRS after CPB[9] or of patients undergoing heart transplantation[10] or surgery for acute infective endocarditis.[11]

Another strategy is to remove from the blood the leukocytes that produce pro-inflammatory factors. Existing leukocyte filters have shown, at best, a transient ability to reduce leukocyte counts in blood after CPB without clinically significant benefits.[12–14] Our previous studies found that short-term–but not long-term–use of a leukocyte filter could attenuate SIRS and reduce infiltration of leukocytes into tissues,[15] but that it could actually cause cellular membrane rupture and cytoplasmic leakage.[16]

Upon activation, inflammatory cells rapidly become adhesive by upregulating adhesion molecules on their surface in a polarized fashion, such that the molecules concentrate in an "adhesion domain" at the terminal end.[17,18] Our novel disposable leukocyte remover leverages this enhanced adhesive ability by incorporating RGD peptide (Arg-Gly-Asp) as a ligand on the membrane, which can stably bind to specific polypeptide groups within the adhesion domain at the terminal end of activated leukocytes,[19] facilitating affinity adsorption. The resulting membrane (Chinese patent CN202310822538.X) is more adhesive and biocompatible than the existing one on which it is based. Furthermore, the membrane is connected at both ends to a hollow support structure, which prevents membrane contact during helical rolling inside the remover and maximizes the membrane surface available for blood contact. The membrane-support structure is integrated into a cylindrical disposable device (Chinese patent CN202211057321.6) that in turn can be integrated into a CPB circuit. Using an extracorporeal circuit, we assessed here the ability of the novel leukocyte remover to selectively remove activated leukocytes from the blood of patients who underwent bypass.

Methods

Extracorporeal Circuit and Patient Blood

A specially treated membrane with a surface area of 50 cm² was produced by the Institute of Blood Transfusion at the Chinese Academy of Medical Sciences in Chengdu, China, then rolled into a cylindrical shape, outfitted at both ends with guide tubes, and placed within a rigid housing (Chengdu Shangyuantai Biotechnology, Chengdu, China; Figure 1A). For the present study, the remover was integrated into an extracorporeal circuit containing a 3-L M/Y reservoir (Jingjing Medical Equipment, Beijing, China) and a Stockert S5 roller pump (Sorin, Mirandola, Italy; Figure 1B).

This is a substudy involving tissue samples obtained within the DIMOCS study, which was approved by the Biomedical Ethics Review Committee of West China Hospital, Sichuan University (No. 2022–262) and registered at Clinicaltrials.gov (NCT05400356). This study was conducted at the Cardiovascular Department of West China Hospital of Sichuan University between December 1, 2022 and March 1, 2023. Patients older than 18 years were included in this study and would not be included into the ongoing large clinical trial. The protocol followed by the guidelines of the Declaration of Helsinki. Written informed consent was obtained preoperatively from all patients and their relatives, and they were informed that they could leave the study at any time for any reason, without consequences.

From seven patients who underwent CPB, blood was harvested from the bypass circuit by flushing normal saline through the arterial, venous and suction tubes as well as the BB841 oxygenator (Medtronic, Minneapolis, USA) and the Type A perfuser (Wego Medical Equipment, Shandong, China). The resulting wash-out fluid (approximately 500 mL) was concentrated to 150 mL using an Xtra hemoconcentrator (Sorin, Mirandola, Italy) and added to the extracorporeal circuit. Blood from each patient was circulated for 10 min at a driving pressure of 100 mmHg and flow rate of approximately 300mL/min, each circulation cycle lasted approximately 30 seconds. The blood was sampled immediately before circulation and after 2.5, 5, 7.5, and 10 min in circulation, corresponding to roughly 5, 10, 15 and 20 cycles. Samples were subjected to routine blood testing on an automated analyzer (Sysmex, Kobe, Japan) as well as flow cytometry to detect the expression of activated cells and molecules (see below). After all seven samples had been circulated, the remover membrane was taken out and analyzed using scanning electron microscopy and immunofluorescence microscopy (see below).

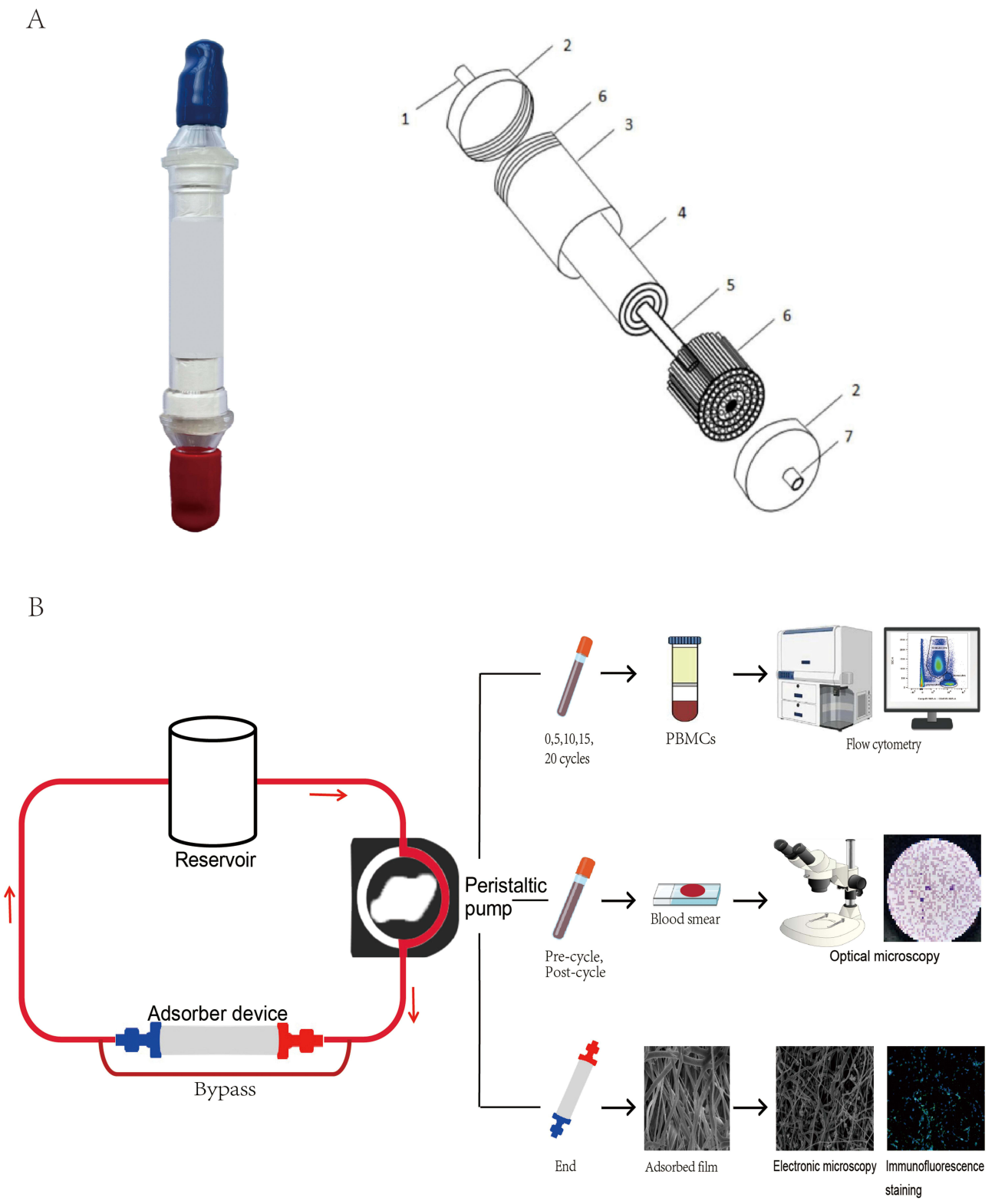

Figure 1 Design of the novel disposable leukocyte remover and its validation in an extracorporeal circuit in vitro. (**A**) Schematic of the remover, showing the outlet (1), cap (2), shell (3), membrane (4), inner support core (5), membrane support structure (6), and inlet (7). (**B**) The remover was integrated into a circuit. Blood from patients who had undergone surgery involving cardiopulmonary bypass was stored in a reservoir and circulated by a roller pump. The blood was sampled immediately before circulation and after 5, 10, 15 and 20 cycles. Activated cells were counted in samples using routine blood analysis and flow cytometry. Morphology of cells was analyzed in smears from blood prepared immediately before circulation and after 20 cycles. Adsorbed cells were analyzed on the membrane after 20 cycles with each of the seven blood samples. **Abbreviation**: PBMCs, peripheral blood mononuclear cells.

https://doi.org/10.2147/JIR.S503575

Flow Cytometry of Activated Leukocytes and Molecules in Blood

Sampled blood was added to 8 mL of 0.85% NH_4Cl solution, allowed to sit at room temperature for 10 min, and centrifuged at 300 ×g at 4 °C for 10 min to lyse the erythrocytes. The supernatant was discarded, and the peripheral blood mononuclear cells (PBMCs) were resuspended in phosphate-buffered saline (PBS) containing 2% fetal bovine serum. The resuspension was centrifuged again at 300 *g* at 4 °C for 10 min, and PBMCs were resuspended in PBS to a concentration of 2×10^6/mL. In separate tubes, equal numbers of PBMCs in aliquots of 100 μL were stained at room temperature in the dark for 30 min with an antibody against an appropriate surface marker to label granulocytes, monocytes, T lymphocytes, B lymphocytes and natural killer cells (Table 1). Samples were centrifuged at 300 *g* at 4 °C for 5 min, and the PBMCs were resuspended in 300 μL PBS, then analyzed on a FACSLyric flow cytometer (BD Biosciences, San Jose, CA, USA) using FlowJo 10.8.1 software (Treestar, Ashland, OR, USA) with manual gating and automated clustering methods. The manual gating was set to exclude debris, dead cells and doublets but retain single live cells for subsequent analysis (Figure 2A). In order to identify and visualize activated

Table 1 Antibodies for Flow Cytometric Identification of Activated Cells in Blood

Fluorophore	Antigen	Commercial Description	Source	ID
Antibodies to characterize granulocytes				
APC-R700	FVS	Fixable Viability Stain 700	BD Pharmingen	564997
BV421	CD123	BV421 Mouse Anti-Human CD123(7G3)	BD Pharmingen	563362
BV510	CD15	BV510 Mouse Anti-Human CD15(W6D3)	BD Pharmingen	563141
BV605	CD45	BV605 Mouse Anti-Human CD45(HI30)	BD Pharmingen	564047
BV786	CD16	BV786 Mouse Anti-Human CD16(B73.1)	BD Pharmingen	741042
FITC	CD14	FITC Mouse Anti-Human CD14(M5E2)	BD Pharmingen	555397
PE	Siglec8	PE anti-human Siglec-8 Antibody	Biolegend	347104
PerCP-Cy5.5	CD54	PerCP/Cyanine5.5 anti-human CD54 Antibody	Biolegend	353120
PE-Cy7	CD11b	PE-Cy7 Mouse Anti-Human CD11b(ICRF44)	BD Pharmingen	557743
APC	CD181	APC Mouse Anti-Human CD181(5A12)	BD Pharmingen	551080
APC-Cy7	CD64	APC-H7 Mouse anti-Human CD64(10.1)	BD Pharmingen	561190
Antibodies to characterize monocytes				
BV421	CD284	BV421 Mouse Anti-Human TLR4 (CD284)(TF901)	BD Pharmingen	564401
BV510	CD40	BV510 Mouse Anti-Human CD40(5C3)	BD Pharmingen	563456
BV605	CD45	BV605 Mouse Anti-Human CD45(HI30)	BD Pharmingen	564047
FITC	CD14	FITC Mouse Anti-Human CD14(M5E2)	BD Pharmingen	555397
PE	HLA-DR	PE Mouse Anti-Human HLA-DR(TU36)	BD Pharmingen	555561
PerCP-Cy5.5	CD80	PerCP-Cy5.5 Mouse Anti-Human CD80 (B7-1)(2D10.4)	BD Pharmingen	567437
PE-Cy7	CD274	PE-Cy7 Mouse Anti-Human CD274(MIH1)	BD Pharmingen	558017
APC	CD163	Alexa Fluor 647 Mouse Anti-Human CD163(GHI/61)	BD Pharmingen	562669
APC-Cy7	CD16	APC-H7 Mouse Anti-Human CD16(3G8)	BD Pharmingen	560195
APC-R700	FVS	Fixable Viability Stain 700	BD Pharmingen	564997
Antibodies to characterize T lymphocytesacterize T cells				
BV421	CD279	BV421 Mouse Anti-Human CD279 (PD-1)(MIH4)	BD Pharmingen	564323
BV510	CD8	BV510 Mouse Anti-Human CD8(SK1)	BD Pharmingen	563919
BV605	CD45	BV605 Mouse Anti-Human CD45(HI30)	BD Pharmingen	564047
FITC	CD38	FITC Mouse Anti-Human CD38(HIT2)	BD Pharmingen	555459
PE	CD69	PE Mouse Anti-Human CD69(FN50)	BD Pharmingen	557050
PerCP-Cy5.5	CD3	PerCP-Cy5.5 Mouse Anti-Human CD3(UCHT1)	BD Pharmingen	560835
PE-Cy7	CD28	PE-Cy7 Mouse Anti-Human CD28(CD28.2)	BD Pharmingen	560684
APC	CD45RO	APC Mouse Anti-Human CD45RO(UCHL1)	BD Pharmingen	559865
APC-Cy7	CD4	APC-Cy7 Mouse Anti-Human CD4(RPA-T4)	BD Pharmingen	557871

(*Continued*)

Table 1 (Continued).

Fluorophore	Antigen	Commercial Description	Source	ID
Antibodies to characterize natural killer cells				
BV421	CD57	BV421 Mouse Anti-Human CD57(NK-1)	BD Pharmingen	563896
BV510	CD335	BV510 Mouse Anti-Human CD335 (NKp46)(9E2/NKp46)	BD Pharmingen	564064
BV605	CD45	BV605 Mouse Anti-Human CD45(HI30)	BD Pharmingen	564047
FITC	Lin(CD19/CD14/ CD123/CD11C/FC)	FITC Mouse Anti-Human CD11c(B-ly6),FITC Mouse Anti-Human CD123(7G3),FITC Mouse Anti-Human CD19(HIB19),FITC Mouse Anti-Human CD14(M5E2),Human BD Fc Block(Fc1.3216)	BD Pharmingen	561355, 558663, 555412, 555397, 564219
PE	CD127	PE Mouse Anti-Human CD127(HIL-7R-M21)	BD Pharmingen	557938
PerCP-Cy5.5	CD3	PerCP-Cy5.5 Mouse Anti-Human CD3(UCHT1)	BD Pharmingen	560835
PE-Cy7	CD56	PE-Cy7 Mouse Anti-Human CD56 (NCAM-1)(B159)	BD Pharmingen	557747
APC	CD314	APC Mouse Anti-Human CD314 (NKG2D)(1D11)	BD Pharmingen	558071
APC-Cy7	CD16	APC-H7 Mouse Anti-Human CD16(3G8)	BD Pharmingen	560195
Antibodies to characterize B lymphocytes				
BV421	CD27	BV421 Mouse Anti-Human CD27(M-T271)	BD Pharmingen	562513
BV510	CD19	BV510 Mouse Anti-Human CD19(SJ25C1)	BD Pharmingen	562947
BV605	CD45	BV605 Mouse Anti-Human CD45(HI30)	BD Pharmingen	564047
FITC	CD38	FITC Mouse Anti-Human CD38(HIT2)	BD Pharmingen	555459
PE	IgG	PE Mouse Anti-Human IgG(G18-145)	BD Pharmingen	555787
PerCP-Cy5.5	IgM	PerCP-Cy5.5 Mouse Anti-Human IgM(G20-127)	BD Pharmingen	561285
PE-Cy7	CD274	PE-Cy7 Mouse Anti-Human CD274(MIH1)	BD Pharmingen	558017
APC	CD80	APC anti-human CD80	Biolegend	305220
APC-Cy7	IgD	APC-H7 Mouse Anti-Human IgD (IA6-2)	BD Pharmingen	561305

cell subpopulations, all live cells were clustered through an automated algorithm (Figure 2B). Subpopulations of leukocytes were plotted onto two-dimensional maps using t-distributed stochastic neighbor embedding (t-SNE)[20] and grouped into phenotypically homogeneous clusters using the "self-organizing map" routine (FlowSOM) in the automated algorithm.[21,22]

Blood Smears

Smears of blood sampled immediately before circulation and after 10 min of circulation were prepared and stained using a G1040 Wright-Giemsa staining kit (Solarbio, Beijing, China). After the smear dried, it was covered with 1 mL of solution A and allowed to sit for 1 min. Then 3 mL of solution B was added and mixed thoroughly with solution A, and the sample was allowed to sit for 3–10 min. The sample was rinsed with water and examined under an Axio Imager A2 LED/DL microscope (Carl Zeiss, Oberkochen, Germany).

Analysis of the Leukocyte Membrane and Adsorbed Cells

After all seven samples had been circulated, the membrane was taken out from the leukocyte remover and some of it was cut into square pieces of 0.5×0.5 cm^2, fixed in 2.5% glutaraldehyde for 1–2 h, rinsed 3 times for 5 min each in PBS containing 2% fetal bovine serum, and dehydrated by soaking sequentially through solutions of 30%, 50%, 75% and 90% anhydrous ethanol in ultrapure water for 5–10 min each time. Finally, the membrane was soaked three times for 5–10 min each time in pure anhydrous ethanol, dried in a CO_2 dryer, attached to a metal stage with conductive adhesive, sputter-coated with ion for 8 min, and examined under an Evo 10 scanning electron microscope (Carl Zeiss, Oberkochen, Germany) at magnifications of 2000–5000.

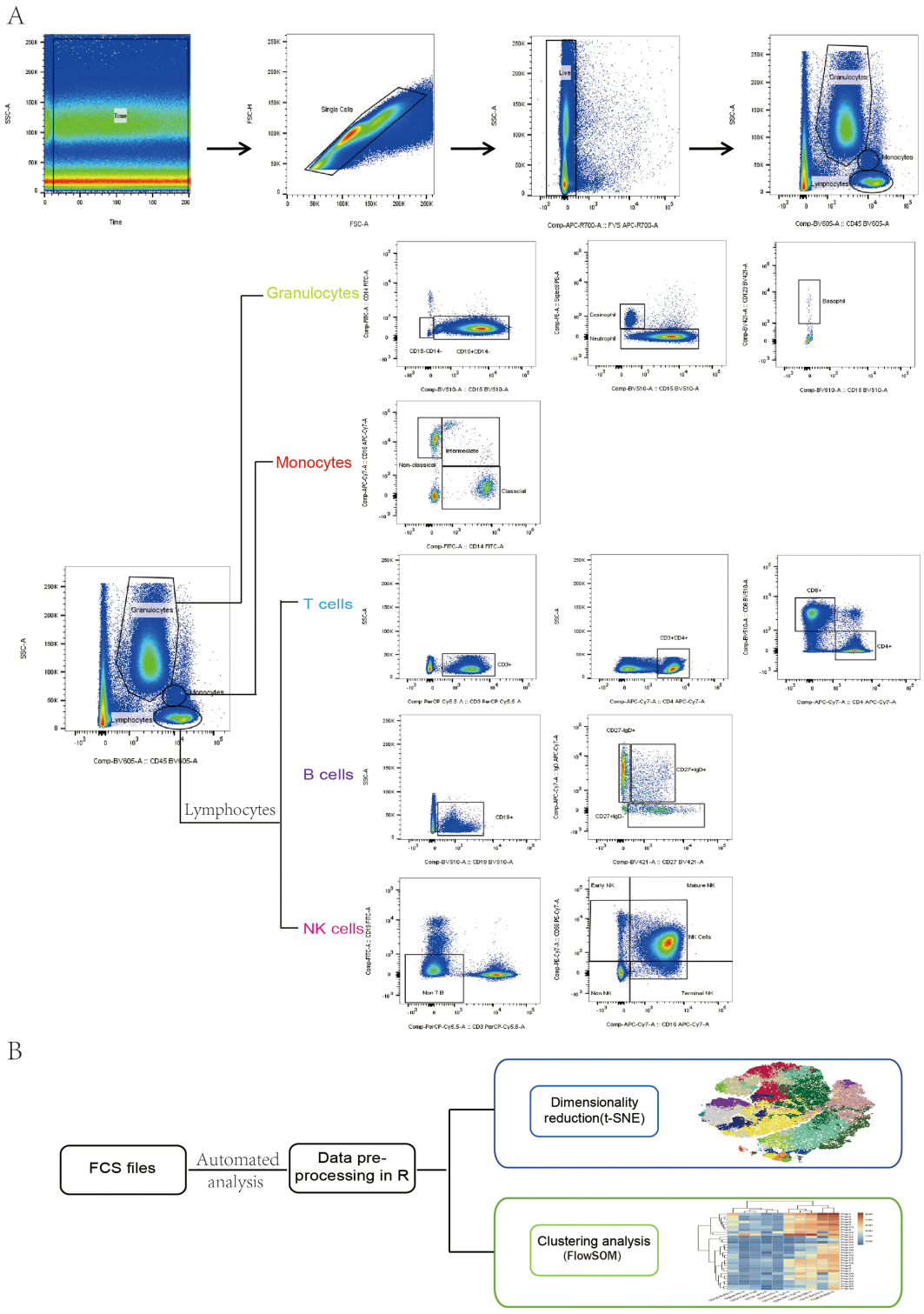

Figure 2 Flow cytometry data analysis. (**A**) Manual gating in FlowJo software, which allowed cell selection based on FSC and SSC in a region of stable flow, while excluding debris, dead cells and doublets. Granulocytes, monocytes and lymphocytes were gated based on expression of CD45, then expression of molecules on the surface of each cell type was analyzed. (**B**) Dimensionality reduction and clustering analysis of flow cytometry data were performed using FlowJo software in conjunction with R in order to identify cell subpopulations whose counts decreased during circulation. Activated cell subsets were visualized in two dimensions using the t-SNE algorithm, with each point corresponding to a cell and their closeness indicating similarity. The t-SNE maps were analyzed using FlowSOM, which automatically clustered cells into phenotypically similar populations, which were color-coded to facilitate analysis of variations in cell abundance during circulation.

Abbreviations: FSC, forward scatter; FCS files, flow cytometry standard files; NK, natural killer; SOM, self-organizing maps; SSC, side scatter; t-SNE, t-distributed stochastic neighbor embedding.

The remaining part of the membrane was cut into square pieces of 1.0×1.0 cm^2, fixed in 2.5% glutaraldehyde for 1–2 h, washed three times with PBS containing 2% fetal bovine serum, blocked for 30 min at room temperature with 5% fetal bovine serum, incubated with anti-CD11b antibody (diluted 1:3000) for 1 h at room temperature or overnight at 4 °C, washed in 2% PBS three times for 5 min each, incubated with secondary antibody for 1 h in the dark at room temperature, again washed in 2% PBS three times for 5 min each, and finally incubated with 4′-6-diamidino-2-phenylindole (DAPI) to stain nuclei. Samples were coverslipped using anti-fade mounting medium and examined under an A1rmp+ two-photon microscope (Nikon, Tokyo, Japan).

Statistical Analysis

Data were analyzed using SPSS 29.0 (IBM, Armonk, NY, USA). Normally distributed data were reported as mean ± standard deviation, and differences were assessed for significance using one-way ANOVA. Skewed data were reported as medians, and differences were assessed using the non-parametric K-samples test. In all cases, differences were considered significant if associated with $P < 0.05$.

Results

Blood for testing the disposable leukocyte remover was taken from seven patients who underwent valve replacement surgery or radiofrequency ablation involving CPB (Table 2).

Changes in Blood Cell Counts

Before circulation, the blood after concentration contained (5.62±1.57)×10^9/L leukocytes, (3.68±1.01)×10^9/L neutrophils, (0.19±0.06)×10^9/L monocytes, (100±25.23)×10^{12}/L platelets, (75±11.00) g/L hemoglobin and (2.52±0.66)×10^{12}/L red blood cells. The counts of each cell type were within normal reference ranges. Within 2.5 min of circulation, during which the blood passed approximately 5 times through the membrane, the leukocyte count dropped by 38%, after which it decreased by approximately 14% every 5 cycles. The levels of hemoglobin and the counts of platelets and red blood cells did not change significantly during 20 cycles (Table 3).

Table 2 Clinicodemographic Characteristics of the Seven Patients Whose Blood Was Used in This Study

Characteristic	Value
Age, year	56 ± 6.68
Height, cm	158.86 ± 3.91
Weight, kg	67.64 ± 10.69
Body mass index, kg/m^2	26.09 ± 4.33
American Society of Anesthesiologists grade III / IV	6 / 1
New York Heart Association grade II / III	4 / 3
Type of surgery	
Mitral valvuloplasty	1
Aortic valvuloplasty	3
Mitral valvuloplasty and aortic valve replacement	2
Wolf Mini-MAZE	1
Preoperative blood analysis	
Red blood cell count, 10^{12} /L	4.98 ± 0.90
Hemoglobin level, g/L	139.42 ± 12.10
Platelet count, 10^9 /L	200.71 ± 53.61
White blood cell count, 10^9 /L	5.97 ± 0.83
Neutrophil count, 10^9 /L	3.41 ± 0.75
Lymphocyte count, 10^9 /L	1.87 ± 0.38
Monocyte count, 10^9 /L	0.43 ± 0.09

Note: Values are n or mean ± SD.

https://doi.org/10.2147/JIR.S503575

Table 3 Cell Counts in Blood as a Function of Number of Cycles in the Disposable Leukocyte Membrane Remover

Cell Type (Unit)	Count After the Indicated No. of Cycles				
	0	5	10	15	20
Leukocytes ($\times 10^9$ /L)	5.62±1.57	3.47±1.18*	2.82±1.00**	2.50±0.91***	2.24±0.75***
Neutrophils ($\times 10^9$ /L)	3.68±1.01	2.27±0.079*	1.77±0.71**	1.45±0.61***	1.23±0.53***
Monocytes ($\times 10^9$ /L)	0.19±0.06	0.09±0.06	0.06±0.04*	0.05±0.02**	0.05±0.02**
Lymphocytes ($\times 10^9$ /L)	1.65±0.53	1.30±0.41	0.93±0.34*	0.94±0.38*	0.91±0.35*
Platelets ($\times 10^9$ /L)	100±25.23	88.86±26.14	83.86±26.26	83±24.39	80±21.20
Red blood cells ($\times 10^{12}$ /L)	2.52±0.66	2.51±0.65	2.50±0.64	2.49±0.63	2.47±0.65
Hemoglobin (g/L)	75±11.00	74.28±11.46	74.29±10.95	74.14±11.44	74.43±11.10

Notes: Values are mean ± SD. 5 cycles took approximately 2.5 min. *p<0.05, **p < 0.01, ***p < 0.001, compared to the cycle 0 count.

Changes in Neutrophils

Flow cytometry showed that counts of neutrophils and of neutrophils expressing CD11b, CD54, CD64 and CD181 decreased by 36–39% during the first 2.5 min, after which they continued to decrease more slowly (Figure 3A). We identified three metaclusters of neutrophils whose counts decreased in t-SNE density plots during the 20 cycles (Figure 3B): metacluster 10 decreased significantly by 46% during the first 2.5 min, after which it declined more slowly; while metaclusters 14 and 17 significantly decreased, respectively, by 72% and 67% after 5 min and more slowly thereafter. All three metaclusters were neutrophil subsets expressing both CD11b and CD64 (Figure 3C).

Changes in Monocytes

Flow cytometry showed that total monocyte count did not decrease significantly until 5 min, when it fell to approximately 33% of the pre-circulation value, after which it decreased by approximately 17% every five cycles. The total decrease affected primarily classical and nonclassical monocytes, because counts of intermediate monocytes did not change significantly during 20 cycles. Flow cytometry also showed that counts of monocytes expressing CD163, CD274 and CD284 decreased by 70–71% during the first 5 min, after which they declined more slowly (Figure 4A). We identified two metaclusters of classical monocytes whose counts decreased in t-SNE density plots during the 20 cycles (Figure 4B): metacluster 9 decreased significantly by 46% during the first 2.5 min, then more slowly thereafter; while metacluster 11 decreased during the 20 cycles, although the decrease did not achieve statistical significance. Both metaclusters were subsets of classical monocytes expressing both CD80 and HLA-DR (Figure 4C).

Changes in Lymphocytes

Counts of total T cells or of T cells expressing CD8 did not decrease significantly during the 20 cycles. In contrast, counts of T cells expressing CD4 decreased significantly by 35% after 5 min (Figure 5A). T lymphocyte t-SNE density maps indicated no reduction in cell subsets densities during circulation (Figure 5B). Counts of all natural killer (NK) cells did not decrease significantly during the 20 cycles, while counts of NK cells expressing CD57 decreased significantly by 39% during the first 2.5 min (Figure 5C). NK cell t-SNE density maps also showed no reduction in cell subsets densities during circulation (Figure 5D). Among B lymphocytes, counts of those expressing CD274 decreased significantly by 36% during the first 2.5 min, counts of those expressing CD38 decreased significantly by 40% in the first 5 min, and counts of those expressing CD80 decreased significantly by 41% during 20 cycles (Figure 5E). B lymphocyte t-SNE density maps revealed no decrease in cell subpopulation density during circulation (Figure 5F).

Effects of Remover on Leukocyte Morphology and Blood Cells

Blood samples before circulation contained neutrophils with ruptured cell membranes and prominent pseudopods, and such cells were nearly absent following circulation, indicating their efficient removal (Figure 6A). Circulation during 20 cycles did not appear to alter the morphology or membrane integrity of lymphocytes or monocytes, nor did it significantly affect levels of hemoglobin or counts of platelets or red blood cells (Figure 6B).

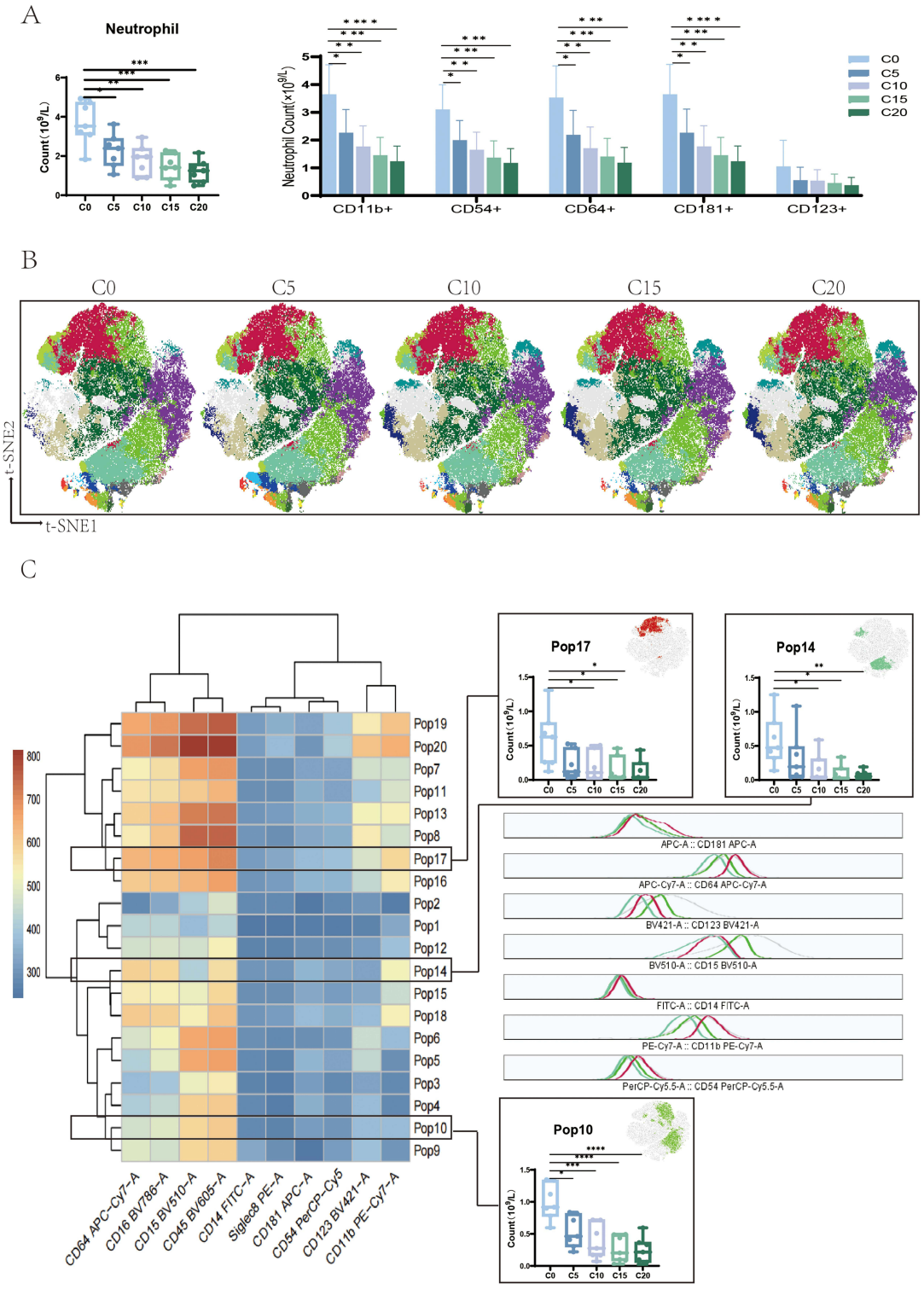

Figure 3 Changes in counts of neutrophils. (**A**) Changes in the counts of total neutrophils and of subsets expressing the indicated surface molecules (n=7). (**B**) Changes in relative abundances of 20 clusters of neutrophils, defined based on t-SNE. (**C**) Metaclusters of neutrophils based on FlowSOM analysis. Rows correspond to metaclusters, while columns correspond to their expression of surface markers (blue, lowest expression; red, highest expression). Metaclusters whose t-SNE density decreased significantly during the 20 cycles are boxed in black. Box plots *above* and *below* on the *right side* of the panel depict metacluster counts as a function of cycle and metacluster position in the t-SNE plot. In the *middle* of the *right side* of the panel, peak expression plots of surface markers are shown for three metaclusters. C0, C5, C10, C15, and C20 indicate: before circulation and after 5, 10, 15 and 20 cycles, respectively. * P < 0.01, ** P < 0.05, ***P < 0.001, ****P < 0.0001 compared to C0.
Abbreviations: Pop, populations; t-SNE,t-distributed stochastic neighbor embedding.

https://doi.org/10.2147/JIR.S503575

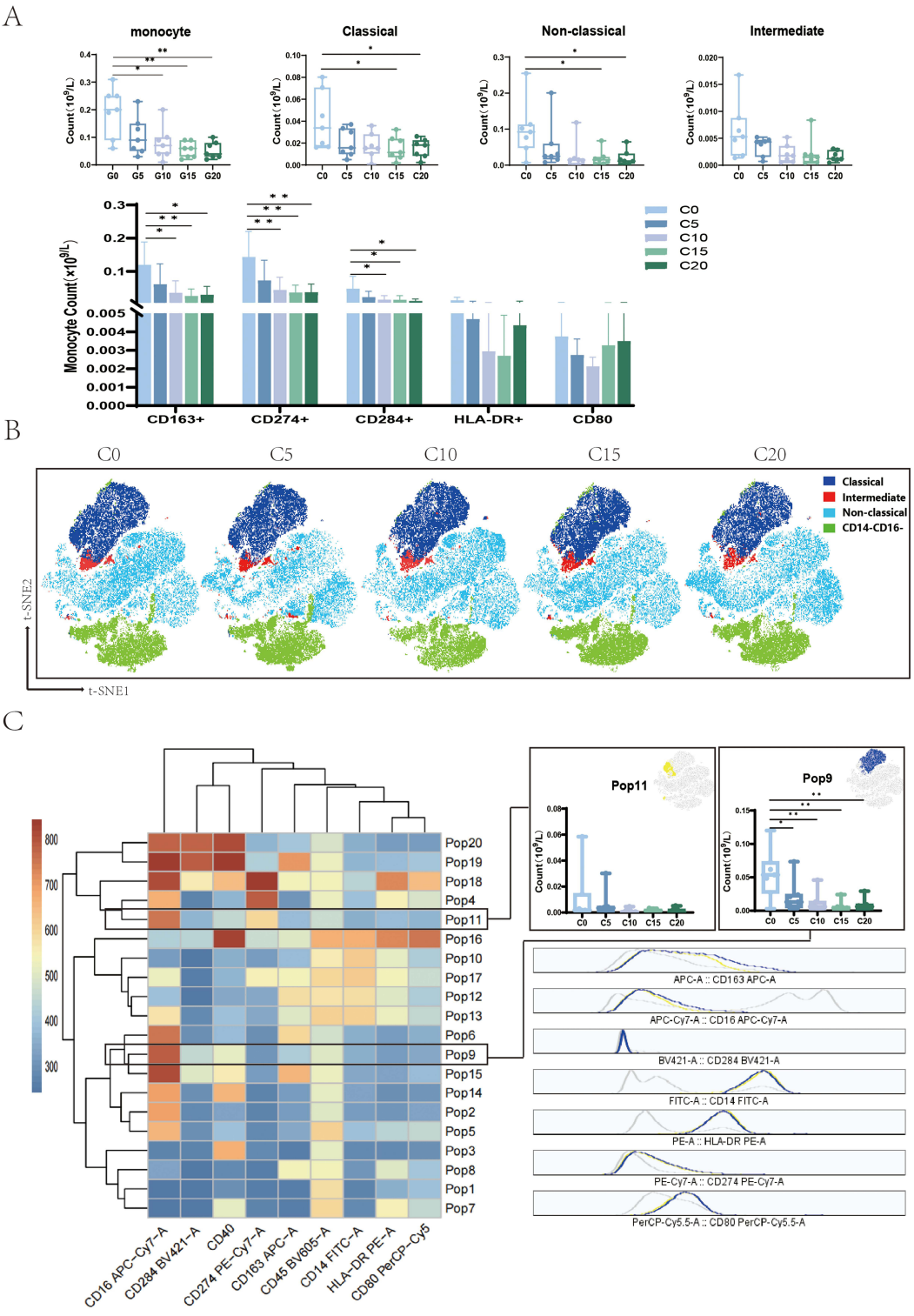

Figure 4 Changes in counts of monocytes. (**A**) Changes in the total number of monocytes and numbers of their surface activation molecules (n=7). (**B**) Changes in relative abundances of 20 clusters of monocytes based on t-distributed stochastic neighbor embedding (t-SNE). (**C**) Metaclusters of monocytes based on FlowSOM analysis. Rows correspond to metaclusters, while columns correspond to their expression of surface markers (blue, lowest expression; red, highest expression). Metaclusters whose t-SNE density decreased significantly during the 20 cycles are boxed in black. Box plots *above* on the *right side* of the panel depict metacluster counts as a function of cycle and metacluster position in the t-SNE plot. In the *below* of the *right side* of the panel, peak expression plots of surface markers are shown for two metaclusters. C0, C5, C10, C15, and C20 indicate: before circulation and after 5, 10, 15 and 20 cycles, respectively. * P < 0.01, ** P < 0.05 compared to C0.

Abbreviations: Pop, populations; t-SNE,t-distributed stochastic neighbor embedding.

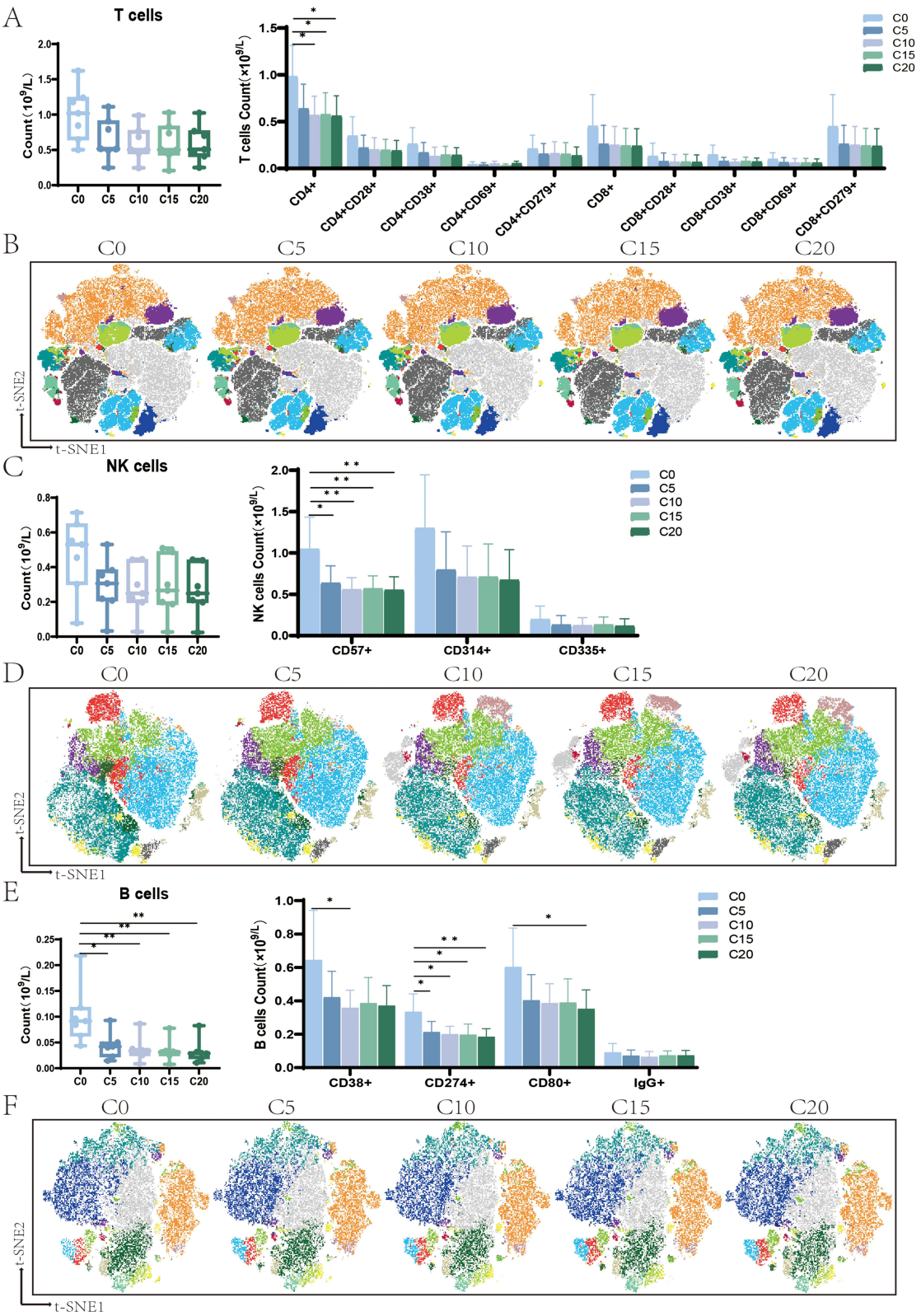

Figure 5 Changes in lymphocytes. (**A**) Changes in the total number of T cells and numbers of their surface activation molecules (n=7). (**B**) Changes in relative abundances of 20 clusters of T cells based on t-distributed stochastic neighbor embedding (t-SNE). (**C**) Changes in the total number of NK cells and numbers of their surface activation molecules (n=7). (**D**) Changes in relative abundances of 20 clusters of NK cells based on t-SNE. (**E**) Changes in the total number of B cells and numbers of their surface activation molecules (n=7). (**F**) Changes in relative abundances of 20 clusters of B cells based on t-SNE. C0, C5, C10, C15, and C20 indicate: before circulation and after 5, 10, 15 and 20 cycles, respectively. * $P < 0.01$, ** $P < 0.05$ compared to C0.

Abbreviations: NK, natural killer; t-SNE, t-distributed stochastic neighbor embedding.

https://doi.org/10.2147/JIR.S503575

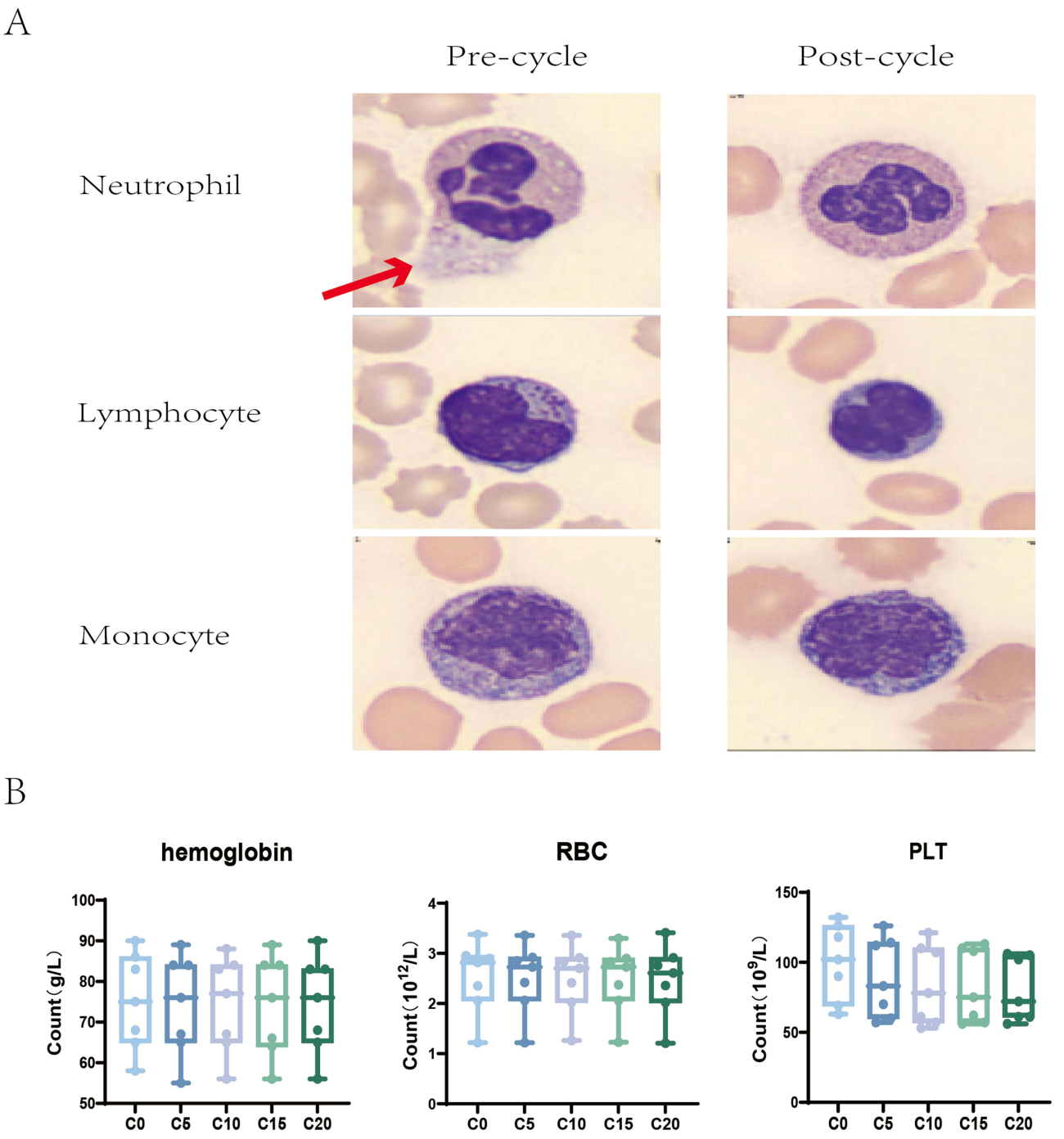

Figure 6 Effect of the remover membrane on morphology of blood cells and platelets. (**A**) Representative photomicrographs of different leukocyte types before circulation (*left*) and after 20 cycles (*right*). The red arrow marks a pseudopod. Magnification, 400×. (**B**) Levels of hemoglobin and counts of red blood cells and platelets during circulation (n=7). C0, C5, C10, C15, and C20 indicate: before circulation and after 5, 10, 15 and 20 cycles, respectively.
Abbreviations: RBC, Red Blood Cell; PLT, platelet.

Analysis of the Remover Membrane

After 20 cycles with each of seven blood samples, the remover membrane appeared smooth and intact and contained numerous intact cells (Figure 7A), which immunostaining revealed to be activated leukocytes (Figure 7B).

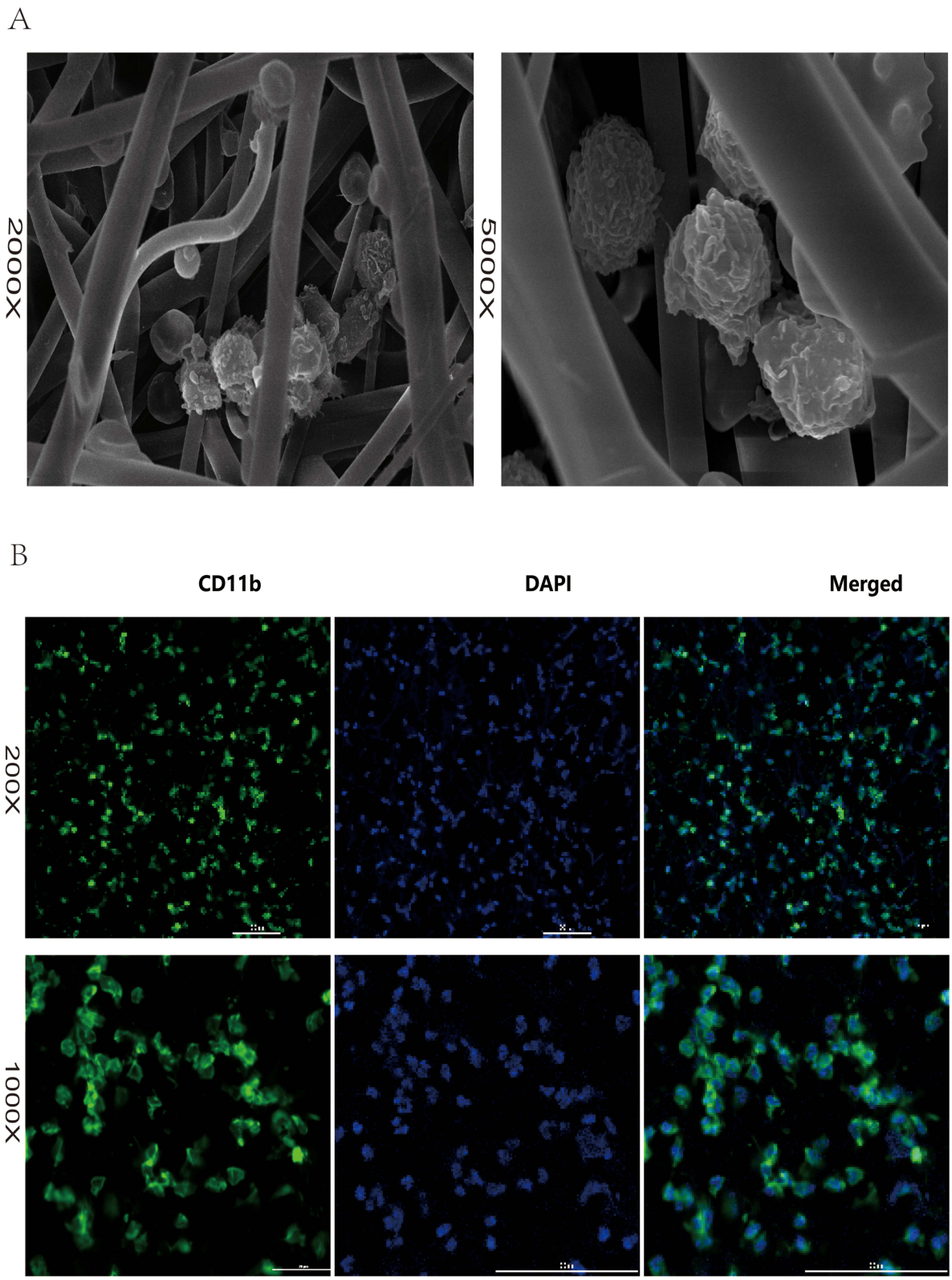

Figure 7 Leukocytes adsorbed onto the remover membrane. The membrane was removed after 20 cycles with each of seven blood samples, then examined using (**A**) scanning electron microscopy; or (**B**) immunostaining against CD11b, a surface marker for activated leukocytes (green), as well as counterstaining of nuclei using DAPI (blue). Magnification factors are indicated at the far left. Scale bar, 100 μm.
Abbreviation: DAPI, 4′-6-diamidino-2-phenylindole.

https://doi.org/10.2147/JIR.S503575

Discussion

Here we describe a novel leukocyte remover and validate it in vitro for its ability to remove, effectively and preferentially, leukocytes that have been activated during CPB. This study justifies further exploration of the novel leukocyte remover membrane as potentially superior to traditional membranes that have demonstrated limited effectiveness in enhancing prognosis following CPB.[23,24]

Activated leukocytes are more adhesive than non-activated ones. Within the first few minutes of circulation, our remover demonstrated a significant ability to remove activated neutrophils, which are among the earliest cells in the bloodstream to participate in inflammatory responses. Levels of activated leukocyte molecules (CD11b, CD54, CD64 and CD181) on neutrophils, consistently declined in abundance with each cycle in circulation. These molecules serve primarily as adhesive and inflammatory chemotactic agents and thereby mediate inflammatory responses and associated tissue damage.[25,26] Elevated levels of CD64, notably, are a diagnostic indicator of SIRS.[27] In our research, we observed a significant reduction in counts of neutrophils expressing these markers during circulation, suggesting that the remover effectively targets activated neutrophils. Immunofluorescence staining revealed a significant accumulation of CD11b+ neutrophils on the membrane, corroborating its adsorption capabilities.

At the same time, the remover had negligible impact on counts of monocytes and lymphocytes during the first few minutes of circulation. Most monocytes and lymphocytes whose counts decreased during circulation were activated, such as monocytes expressing CD163 and NK cells expressing CD57. Expression of CD163, a receptor involved in inflammation and hemoglobin clearance, increases during inflammatory responses, making it a reliable marker of inflammation.[28] Lipopolysaccharide binds to a receptor comprising Toll-like receptor-4 (TLR4/CD284) and CD14 on the surface of monocytes to activate them.[29] Monocytes, as well as macrophages, express PD-L1 (CD274), a ligand for PD-1 (CD279), and levels of PD-L1 on monocytes are associated with risk of mortality in sepsis patients.[30] CD57 serves as a marker of NK cell maturity, potentially indicating terminal differentiation.[31] Modest reduction of monocytes and lymphocytes during circulation, we propose that, the adsorptive removal of these cells during circulation may occur via the adhesion molecules CD11b and CD62L, which are expressed at low levels on the surface even in the absence of activation.[32] Applying the leukocyte remover for shorter than 2.5 min may help minimize adverse impacts on immune cell counts. During this short period, our remover appears to target preferentially activated leukocytes, particularly neutrophils, while minimally affecting other leukocyte subsets, potentially making it superior to previously described membranes.[16] In this way, the remover may help mitigate the postoperative rise in levels of inflammatory cytokines without compromising the body's immune function.[33,34]

Another reason to limit how long the remover is applied is to prevent the activation and lysis of leukocytes similar to that reported after prolonged application of a previously described leukocyte membrane.[16] Such activation and lysis increase risk of inflammatory responses. In our experiments, the bulk of neutrophil removal occurred within the first 2.5 min, corresponding to approximately 5 cycles through the circulatory loop. Future work should optimize the cycling time to maximize leukocyte removal and improve safety simultaneously.

We did not observe substantial effects of the remover on counts or morphology of platelets or red blood cells, implying minimal interference with coagulation or oxygenation capacity of the blood. Furthermore, the blood cells that were not adsorbed showed similar morphology before and after passing over the membrane. Microscopic examination of the cellular morphology on the adsorptive membrane revealed that white blood cells remained intact, with no exposed nuclei detected, implying negligible leakage of proteases and pro-inflammatory substances.

We attribute the greater efficacy and selectivity of our membrane to the fact that blood flows *over* it rather than *through* it as in previously described membranes. Our membrane leverages the strong adhesiveness of activated leukocytes. Additionally, the hollow support structure of the membrane ensures that blood makes contact with both sides of the membrane as it flows through the remover, maximizing adsorption efficiency.

Our findings should be interpreted with caution given that concentrated residual blood may not behave identically to normal human blood and may differ significantly in concentrations of proteins and coagulation factors. This difference might affect the equivalence of concentrated blood to whole blood removal. Another limitation of our study is that we used a membrane with a surface area of only 50 cm^2, raising the question of whether the disposable remover will function similarly when scaled up for clinical use. Lastly, this study focused on ex vivo blood research, so in vivo performance may differ significantly. For example,

leukocytes from bone marrow constantly enter the blood during CPB within the body, which was not the case in our experiments. Despite these limitations, our results justify further development and optimization of our novel disposable leukocyte remover to improve prognosis of patients after CPB.

Conclusion

Our novel disposable leukocyte remover can preferentially remove activated neutrophils from ex vivo blood of patients who underwent CPB, with minimal impact on other leukocyte subsets and blood components. These findings highlight the remover's potential to reduce inflammation-related complications after bypass, justifying further investigation in larger studies.

Ethics Approval and Consent to Participate

The study protocol was approved by the Biomedical Ethics Review Committee of West China Hospital, Sichuan University (2022-262), and the study was conducted in line with the Declaration of Helsinki. All patients gave written informed consent before enrollment.

Acknowledgments

We thank Creaducate Consulting GmbH (Munich, Germany) for linguistic assistance during the preparation of this manuscript.

Author Contributions

All authors made a significant contribution to the work reported, whether in the conception, design or execution of the study or in the acquisition, analysis or interpretation of the data; took part in drafting, revising or critically reviewing the manuscript; approved the submitted version of the manuscript and the receiving journal; and agree to be held accountable for all aspects of the work.

Funding

This study was supported by the 1•3•5 Project for Disciplines of Excellence from West China Hospital, Sichuan University (grant 2017-120).

Disclosure

The authors report no conflicts of interest related to this work.

References

1. Paparella D, Yau TM, Young E. Cardiopulmonary bypass induced inflammation: pathophysiology and treatment. An update. *Eur J Cardiothorac Surg*. 2002;21(2):232–244. doi:10.1016/S1010-7940(01)01099-5
2. Warren OJ, Smith AJ, Alexiou C, et al. The inflammatory response to cardiopulmonary bypass: part 1—mechanisms of pathogenesis. *J Cardiothorac Vasc Anesthesia*. 2009;23(2):223–231.
3. Bronicki RA, Hall M. Cardiopulmonary bypass-induced inflammatory response: pathophysiology and treatment. *Pediatr Crit Care Med*. 2016;17(8 Suppl):S272–S278. doi:10.1097/PCC.0000000000000759
4. Rossaint J, Berger C, Aken HV, et al. Cardiopulmonary bypass during cardiac surgery modulates systemic inflammation by affecting different steps of the leukocyte recruitment cascade. *PLoS One*. 2012;7(9):e45738. doi:10.1371/journal.pone.0045738
5. Clive R. Landis.Redefining the systemic inflammatory response. Seminars in Cardiothoracic & Vascular Anesthesia. 2009.
6. Kristeller JL, Jankowski A, Reinaker T. Role of corticosteroids during cardiopulmonary bypass. *Hosp Pharm*. 2014;49(3):232–236. doi:10.1310/hpj4903-232
7. Fry DE. Sepsis, systemic inflammatory response, and multiple organ dysfunction: the mystery continues. *Am Surg*. 2012;78(1):1–8. doi:10.1177/000313481207800102
8. Basu R, Pathak S, Goyal J, et al. Use of a novel hemoadsorption device for cytokine removal as adjuvant therapy in a patient with septic shock with multi-organ dysfunction: a case study. *Indian J Crit Care Med*. 2014;18(12):822–824. doi:10.4103/0972-5229.146321
9. Poli EC, Alberio L, Bauer-Doerries A, et al. Cytokine clearance with CytoSorb during cardiac surgery: a pilot randomized controlled trial. *Critical Care*. 2019;23(1):108. doi:10.1186/s13054-019-2399-4
10. Santer D, Miazza J, Koechlin L, et al. Hemoadsorption during cardiopulmonary bypass in patients with endocarditis undergoing valve surgery: a retrospective single-center study. *J Clin Med*. 2024;10(4):564. doi:10.3390/jcm10040564

11. Bernardi MH, Rinoesl H, Dragosits K, et al. Effect of hemoadsorption during cardiopulmonary bypass surgery - a blinded, randomized, controlled pilot study using a novel adsorbent. *Crit Care*. 2016;20:96. doi:10.1186/s13054-016-1270-0
12. Gu JY, Engels GE, Van Oeveren W. Leukocyte depletion during extracorporeal circulation allows better organ protection but does not change hospital outcomes. *Ann Thorac Surg*. 2011;91(2):534–540. doi:10.1016/j.athoracsur.2010.09.077
13. Bechtel JM, Mühlenbein S, Eichler W, et al. Leukocyte depletion during cardiopulmonary bypass in routine adult cardiac surgery. *Interact Cardiovasc Thorac Surg*. 2011;12(2):207–212. doi:10.1510/icvts.2010.246868
14. Ilmakunnas M, Pesonen EJ, Ahonen J, et al. Activation of neutrophils and monocytes by a leukocyte-depleting filter used throughout cardiopulmonary bypass. *J Thorac Cardiovasc Surg*. 2005;129(4):851–859. doi:10.1016/j.jtcvs.2004.07.061
15. Zhao-Qiong Z, Yi-Bin Y, Hong Z, et al. The influence of leukocyte depletion filter-LD-1 on leukocytes, IL-6, MPO and the pathologic changes of myocardic tissues during cardiopulmonary bypass. Sichuan da xue xue bao. *Yi Xue Ban*. 2005;36(3):429–431.
16. Tang J, Tao K, Du L, et al. Long-term leukocyte filtration should be avoided during extracorporeal circulation. *Mediators Inflamm*. 2013;2013:612848. doi:10.1155/2013/612848
17. Patel KD, Cuvelier SL, Wiehler S. Selectins: critical mediators of leukocyte recruitment. *Semin Immunol*. 2002;14(2):73–81. doi:10.1006/smim.2001.0344
18. Ebnet K, Kummer D, Steinbacher T, Singh A, Nakayama M, Matis M. Regulation of cell polarity by cell adhesion receptors. *Semin Cell Dev Biol*. 2018;81:2–12. doi:10.1016/j.semcdb.2017.07.032
19. Chen W, Harbeck MC, Zhang W, Jacobson JR. MicroRNA regulation of integrins. *Transl Res*. 2013;162(3):133–143. doi:10.1016/j.trsl.2013.06.008
20. Zhou Y, Sharpee T. Using global t-SNE to preserve inter-cluster data structure. 2018.
21. Van Gassen S, et al. FlowSOM: using self-organizing maps for visualization and interpretation of cytometry data. 2024.
22. Quintelier K, Couckuyt A, Emmaneel A, et al. Analyzing high-dimensional cytometry data using FlowSOM. *Nature Protocols*. 2024.
23. Grace LA, Joseph S, Joel D, et al. Can leucocyte depletion reduce reperfusion injury following cardiopulmonary bypass? *Interact Cardiovasc Thorac Surg*. 2017;2:232.
24. Rubino AS, Serraino GF, Mariscalco G, et al. Leukocyte depletion during extracorporeal circulation allows better organ protection but does not change hospital outcomes. *Ann Thorac Surg*. 2011;91(2):534–540.
25. Skogby M, Mellgren K, Mellgren G, et al. Induced cell trauma during in vitro perfusion: a comparison between two different perfusion systems. *Artif Organs*. 1998;22(12):1045–1051. doi:10.1046/j.1525-1594.1998.06064.x
26. Bui TM, Wiesolek HL, Sumagin R. ICAM-1: a master regulator of cellular responses in inflammation, injury resolution, and tumorigenesis. *J Leukoc Biol*. 2020;108(3):787–799. doi:10.1002/JLB.2MR0220-549R
27. Groselj-Grenc M, Ihan A, Derganc M. Neutrophil and monocyte CD64 and CD163 expression in critically ill neonates and children with sepsis: comparison of fluorescence intensities and calculated indexes. *Mediators Inflamm*. 2008;2008:202646. doi:10.1155/2008/202646
28. Møller HJ, Peterslund NA, Graversen JH, et al. Identification of the hemoglobin scavenger receptor/CD163 as a natural soluble protein in plasma. *Blood*. 2002;99(1):378–380. doi:10.1182/blood.V99.1.378
29. Winkler MS, Rissiek A, Priefler M, et al. Human leucocyte antigen (HLA-DR) gene expression is reduced in sepsis and correlates with impaired TNFα response: a diagnostic tool for immunosuppression? *PLoS One*. 2017;12(8):e0182427. doi:10.1371/journal.pone.0182427
30. Shao R, Fang Y, Yu H, et al. Monocyte programmed death ligand-1 expression after 3-4 days of sepsis is associated with risk stratification and mortality in septic patients: a prospective cohort study. *Crit Care*. 2016;20(1):124. doi:10.1186/s13054-016-1301-x
31. Lopez-Vergès S, Milush JM, Pandey S, et al. CD57 defines a functionally distinct population of mature NK cells in the human CD56dimCD16+ NK-cell subset. *Blood*. 2010;116(19):3865–3874. doi:10.1182/blood-2010-04-282301
32. Stefanou DC, Asimakopoulos G, Yagnik DR, et al. Monocyte Fc gamma receptor expression in patients undergoing coronary artery bypass grafting. *Ann Thorac Surg*. 2004;77(3):951–955. doi:10.1016/j.athoracsur.2003.09.026
33. Xing Z, Han J, Hao X, et al. Immature monocytes contribute to cardiopulmonary bypass-induced acute lung injury by generating inflammatory descendants. *Thorax*. 2017;72(3):245. doi:10.1136/thoraxjnl-2015-208023
34. Rodríguez-López JM, Iglesias-González JL, Lozano-Sánchez FS, et al. Inflammatory response, immunosuppression and arginase activity after cardiac surgery using cardiopulmonary bypass. *J Clin Med*. 2022;11(14):4187. doi:10.3390/jcm11144187